World Journal of Advanced Research and Reviews
eISSN: 2581-9615 CODEN (USA): WJARAI
Cross Ref DOI: 10.30574/wjarr
Journal homepage: https://wjarr.com/

(RESEARCH ARTICLE)

Check for updates

Evaluate the hemodynamic factors' effects on stenosed arteries with the Carreau model

Zahraa Ahmed Hamza [1,*], Mohammed Ghalib Al-Azawy [1], Alaa Ahmed Alkinani [2], Ahmed A Y Al-Waaly [1] and Ahmed Basheer [2]

[1] *Department of Mechanical Engineering, Wasit University, Wasit, Iraq.*
[2] *Al-Zahraa teaching Hospital, Wasit, Iraq.*

World Journal of Advanced Research and Reviews, 2022, 16(01), 622–631

Publication history: Received on 11 September 2022; revised on 15 October 2022; accepted on 18 October 2022

Article DOI: https://doi.org/10.30574/wjarr.2022.16.1.1050

Abstract

One of the main causes of death is atherosclerosis so, in this work, two models of stenosed arteries have been executed numerically to assess the hemodynamic effects caused by flow disruptions. Using Computational Fluid Dynamics (CFD) to provide information to the public, particularly surgeons, and assist them in reducing the risk of stenosis. Star-CCM+ software was used to perform CFD techniques such as steady, turbulent, and non-Newtonian (Carreau) and was applied at two different flow rate conditions. Using the blood flow velocity, vorticity, strain rate, and wall shear stress for identifying the plaque-affected section of the arteries, the results showed that in the stenosed areas there is a high blood flow velocity due to the smaller lumen diameter, and a recirculation region was also identified immediately after the stenosed part, resulting in increased plaque development.

Keywords: Atherosclerosis; Stenosis; Turbulent; Carreau; Vorticity

1. Introduction

The disease atherosclerosis is what alters the normal behaviour of flow of blood in coronary arteries. As a result of stenosis (the build-up of lipids, cholesterol, and other chemicals) on the internal surfaces of coronary arteries, one of the main causes of death is atherosclerosis. According to a number of studies, the bifurcation, branching, and curves of vessels are preferentially where stenosis begins and progresses [1]. Although it is impossible to directly measure the variation in wall shear stress and disturbed flow variations in coronary arteries, computational fluid dynamic (CFD) simulation offers an alternative method for assessing the shear stresses and detecting the early stages of stenosis [2]. In recent years, sophisticated computers and numerical techniques have been used to build computational fluid dynamic modelling of stenotic flow [3]. Numerous research [4][5] reported the impact of varied stenosis forms, curvature angles, and branch angles on physiological parameters. The blood flow behaviour was believed to be laminar in several previously published research [6], and others [7][8] investigated the transition from laminar to turbulence and the non-Newtonian impacts of blood in an ideal stenosed artery with a single stenosis. In several earlier investigations [9][10], experimental analysis of the flow behaviour in the downstream zone of idealized stenosed models was conducted.

Chaichana et al.[2] simulated the impact of stenosis on the physiological parameters of the patient specific left coronary heart model. In models both with and without stenosis, the pressure difference and velocity distribution were estimated and compared. They discovered that the stenosis has a significant pressure gradient and the post-stenosis has a low velocity.

* Corresponding author: Zahraa Ahmed Hamza
Department of Mechanical Engineering, Wasit University, Wasit, Iraq.

The left coronary artery's hemodynamic impact of diverse plaque configuration types was evaluated by Chaichana et al. [11]. For the plaque geometries, they computed velocity, wall shear stress, and pressure difference. They discovered a sort of plaque configuration involving the plaque location in all three left coronary branching to have the largest velocity and pressure gradient.

In an actual patient specific left coronary heart model, the effects of different degrees of stenosis on pressure, velocity, and wall shear stress were investigated by Kamangar et al. [12].

Additionally, the researchers found that there were significant issues with blood flow following stenosis, particularly in relation to non-Newtonian effects [13][14][15]. In order to investigate the effects of wall shear stress inside various arteries, Johnston et al.[16] employed five distinct blood viscosity formulas (Walburn-Schneck, Carreau, Power law , Generalized power law model and Casson) in addition to the Newtonian model. Using these models, the authors looked at local and global non-Newtonian important factors and recommended using the non-Newtonian model to get a good assessment of wall shear stress at low shear. Additionally, Molla and Paul [17] employed five distinct non-Newtonian (Power low, Carreau, Cross, modified-Casson and Quemada), the levels of these models' effects on the pressure drop and wall shear stress were assessed by the authors in this study. The findings demonstrated that when the impacts of blood viscosity estimates were taken into account, the decrease in shear stress was greater.

Additionally, Halder et al. [18] examined the blood flow within artery stenosis utilizing a variety of pulsatile flow variations and various inlet velocity profiles using the Carreau Yasuda model. The authors compared Newtonian and non-Newtonian models' velocity fields, vortex distribution, wall shear stress, and strain rate, found that there were substantial discrepancies between all these models.

The aim of the present work is to evaluate the hemodynamic effects caused by flow disruptions in stenosed arteries by using the Carreau model.

2. Methodology

2.1. Physics model

In the present work, two models of stenosed arteries were performed as illustrated in figure 1. The area of stenosis for these cases was 30% and 60%. The length of stenosis, which is 6 mm in two cases, is constant, and the artery's diameter is 3 mm as illustrated in figure 1, which presents the geometry of the cases and the area of stenosis (AS), which is represented by the formula [19]

$$AS\ \% = (1 - D_s/D_n\ ) \times 100\% \ldots\ldots\ldots\ldots\ldots\ldots\ldots (1)$$

Where;
D_n is the artery diameter
D_s is the stenoses diameter

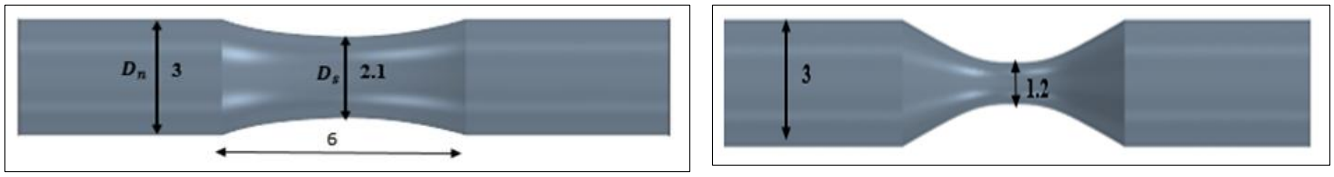

30% stenosed artery 60% stenosed artery

Figure 1 Geometry of models (all dimension's in mm)

2.2. Numerical description

A mathematical modelling of the 3D computational geometry of a stenosis artery is produced using the commercial CFD software STAR-CCM+ 2021.2.1 (16.04.012-R8) [20] In this program , the stable Navier-Stokes equations are solved numerically using finite volume methods [21], as demonstrated below:

$$\frac{\partial u_i}{\partial x_i} = 0 \ldots\ldots\ldots\ldots\ldots\ldots\ldots\ldots (2)$$

$$\rho u_j \frac{\partial u_i}{\partial x_j} = -\frac{\partial p}{\partial x_i} + \frac{\partial}{\partial x_j}\left[\mu(s)\frac{\partial u_i}{\partial x_j} - \overline{u_i u_j}\right] \ldots\ldots\ldots\ldots(3)$$

Here u_i is the change in velocity, u_i = (u , v, w), is the Cartesian coordinate, x_i = (x, y, z); while p is the pressure and ρ is the density (1060kg/ m^3) , $\overline{u_i u_j}$ is the Reynolds stress tensor, $\mu(s)$ is the blood viscosity, which is calculated from the shear rate tensor [20] as follows:

$$|S| = \sqrt{2\, S_{ij}\, S_{ij}}$$

$$\text{Where; } S_{ij} = \frac{1}{2}\left(\frac{\partial u_i}{\partial x_j} + \frac{\partial u_j}{\partial x_i}\right) \ldots\ldots\ldots(4)$$

To study at the spatially mesh resolution requirement for three-dimensional simulations, a number of different meshes must be generated. CFD mesh generating software based on STAR-CCM+ [20] was utilized to create the CFD meshes in this investigation.

Because the computing time increases as the mesh size grows, it's critical to choose an appropriate number of cells to record the flow's properties within the device. To evaluate this, five separate meshes were created in the current investigation using STAR-CCM+ v.12.02.011[20] to recognize the resolution of the spatial mesh, as shown in table 1.

Table 1 Information of the mesh

Mesh	**M1**	**M2**	**M3**	**M4**	**M5**
Number of cells	125466	326726	859145	1092156	1377140

A polyhedral mesh was used for the CFD model, which is suited for complex flow applications. The boundary layer was resolved using a prism layer made up of four layers. The grid is generated at 60% of the stenoses artery, as illustrated in figure 2.

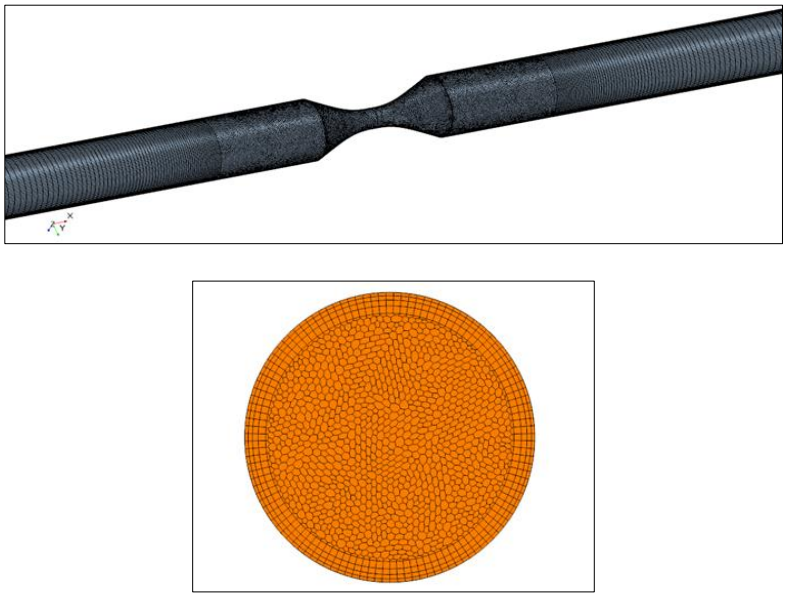

Figure 2 Mesh configurations displaying the prism layer

In addition, Figure 3 shows the behavior of axial velocity down a horizontal line across a stenosis region (at 60% stenoses artery), demonstrating a grid-independency test. The velocity forecasts for meshes M4 and M5 are roughly comparable to the other three meshes, as illustrated in this graph. As a result, the mesh M4 (1092156cells) is selected to represent the fluid characteristics across the model for the following simulation.

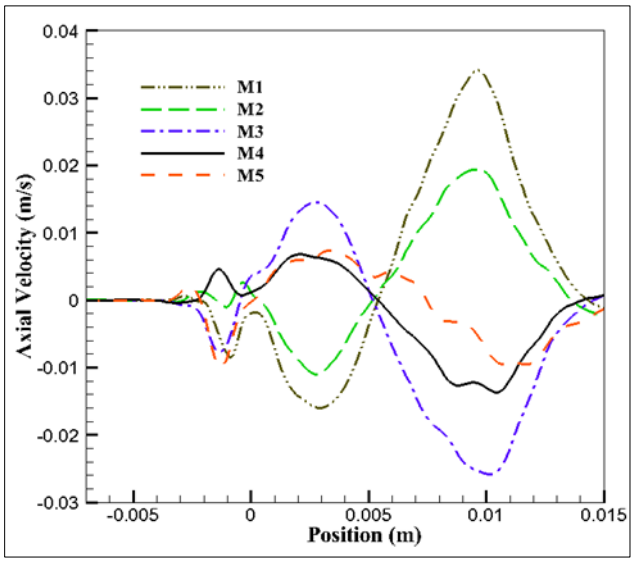

Figure 3 Plot of Axial velocity through a horizontal centreline

2.3. Assumptions and boundary conditions

The present flow simulation was assumed to be steady, incompressible, turbulent, and non-Newtonian fluid flow. In addition, the boundary conditions were utilized as follows:

- In all simulations, the inlet velocity was calculated using two conditions of flow rate value as shown in table 2
- There was no slipping on the walls.
- A relative zero pressure was applied at the outlet.

Table 2 Conditions that applied at the inlet [22]

Condition	Condition 1:at rest	Condition 2:at exercise
Flow rate (units)	85 ml/min	255 ml/min
Velocity at the inlet (unit)	0.2 m/s	0.6 m/s

2.4. Modelling of blood rheology and turbulence model

According to [13]and [23], blood is a non-Newtonian fluid, yet blood flow in a large artery channel can be represented as a Newtonian fluid. Like a result, the Navier-Stokes equations of motion are suitable for investigating the mechanics of blood flow across a stenosis.

The relationship between shear stress and shearing strain rate in non-Newtonian fluids is not linear. As in the case of blood, this means that viscosity can fluctuate as a function of shear rate. The power law model, Walburn-Schneck model, Carreau model, Casson model, Cross, Bingham model, and generalized Power model are all models for non-Newtonian fluids. These models are known as modified Newtonian models since they are based on experimental evidence.in the present work we used the Carreau model. The Carreau model produces more realistic findings when simulating blood flow, and it is widely used in hemodynamic studies [17] when compared to other non-Newtonian models.

The Carreau model is shaped like this [24]:

$$\boldsymbol{\mu}(|\boldsymbol{S}|) = \boldsymbol{\mu}_{\infty} + (\boldsymbol{\mu_0} - \boldsymbol{\mu}_{\infty})[\mathbf{1} + (\boldsymbol{\lambda S})^{\mathbf{2}}]^{(\boldsymbol{n-1})/2} \quad \ldots\ldots\ldots\ldots\ldots (5)$$

The information for the variables that are mentioned in the previous equation is found in Table 3.

Table 3 Parameters used with Carreau approach [24]

Blood viscosity at zero shear rate, $\mu 0$	Blood viscosity at infinite shear rate, $\mu\infty$	The relaxation time, λ	The constant model, n
0.056 Pa s	0.00345 Pa s	3.313	0.3568

Because stenosis can cause the flow to become turbulent and produce recirculation zones, turbulence modeling is important in hemodynamics examinations. Predicting the actual challenges brought on by this change in arterial area requires taking the effect of turbulence within vessels with narrowing into consideration. Because of its improved capabilities, particularly with low Reynolds numbers, the elliptic blending Reynold stress model was selected in this work [25][26].

3. Results and discussion

3.1. Examination of flow field

3.1.1. Validation with previous work

Validation with experimental data is an essential step for estimating the numerical simulation's confidence level. The current numerical simulation has been validated using experimental data from the Food and Drug Administration (FDA) nozzle model [27]. The axial velocity that is presented in figure 4 of the geometry along a horizontal axis for the Non-Newtonian Carreau model. This figure shows high compatibility with the experimental findings of [27]. Thus, the maximum percent error between the simulation result model of viscosity (Carreau) and the experimental data that is found from the result of [27] is 2.5%.

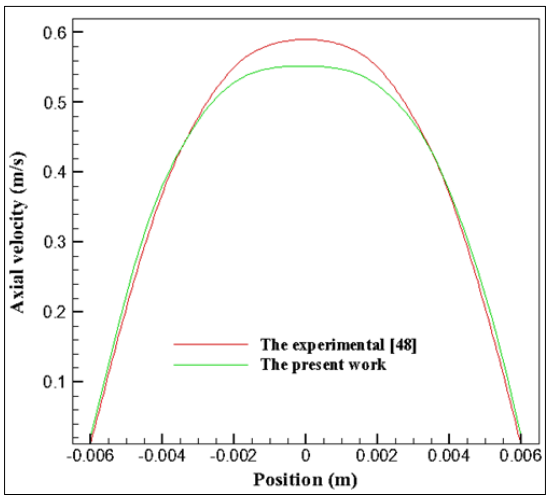

Figure 4 The results of the STAR-CCM+ program and the experimental data from[27] at x=-30$\boldsymbol{mm}$

3.1.2. Velocity filed

One of the most essential indications for identifying the plaque-effected section of the coronary arteries is the velocity of blood flow as shown in figure 5, which indicated the contour of velocity magnitude in m/s of different cases of area stenoses at different conditions.

From figure 5, the velocity across the stenosed portion was found to be much higher. A recirculation region was also identified immediately after the stenosed part that results in increased plaque development.

In the stenosed areas, there is a high blood flow velocity. Due to the smaller lumen diameter, the increased velocity communicates greater blood flow resistance and reduced blood flow. This information could be extremely useful to medical professionals in locating hotspots wherein blood is like to collect. Furthermore, blood flow in the plaque-effected region is restricted, resulting in an imbalance in oxygen demand and supply in the tissue. Another of the main

reasons for chest discomfort and other symptoms of coronary heart disease is the diminished oxygen delivery to the surrounding tissues.

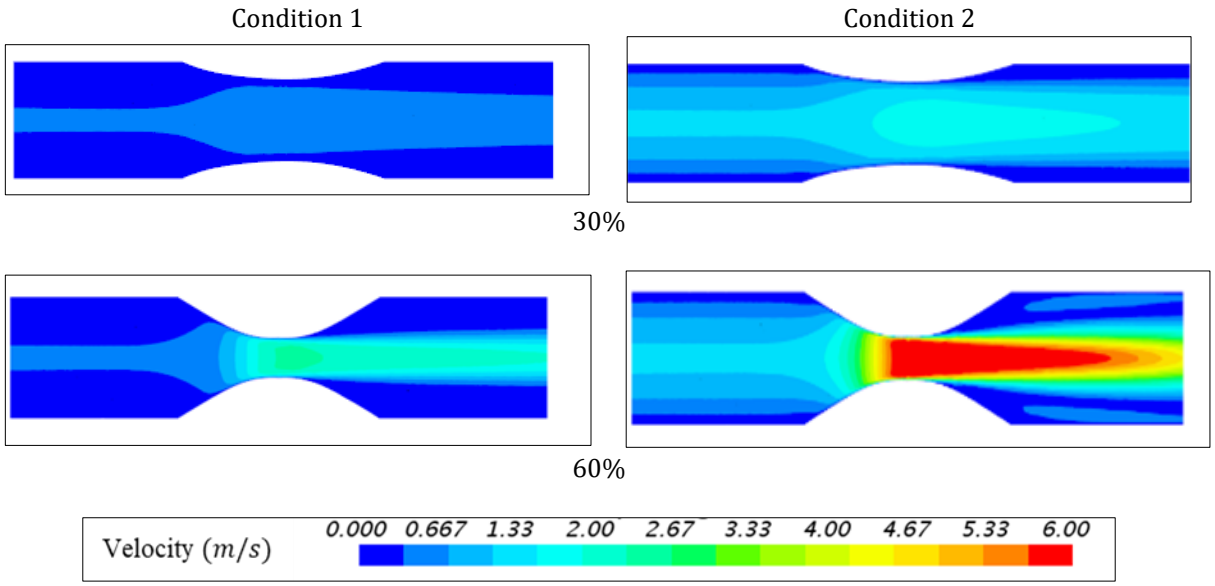

Figure 5 Contour of velocity magnitude at mid plane

3.1.3. Vorticity

Vorticity is a term that characterizes the local spinning action of a fluid and is strongly influenced by viscosity. As defined in equation below [28].

$$|\omega| = \sqrt{2\omega_i\omega_i} \dots\dots\dots\dots\dots (6)$$

Where;

$$\omega_i = \epsilon_{ijk} \frac{\partial u_k}{\partial u_j} \dots\dots\dots\dots\dots\dots (7)$$

Where;
ω_i is the vorticity vector
ϵ_{ijk} is the Levi-Civita cyclic operator

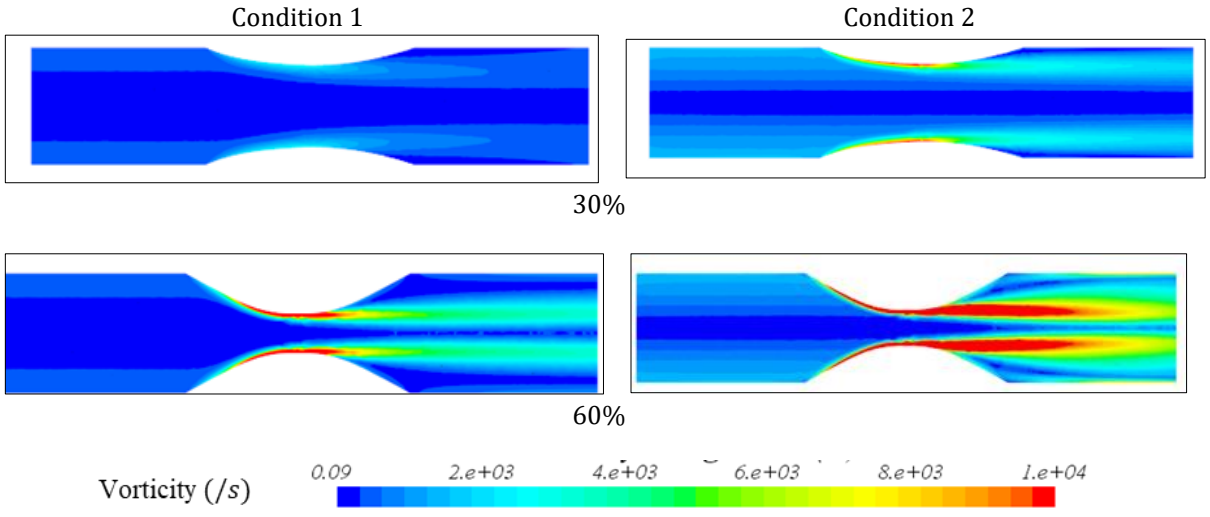

Figure 6 Contour of vorticity at mid plane

It should be mentioned that a lesser vorticity means less blood particle rotation, which is one of the variables that might cause blood to accumulate, which can lead to thrombosis. The flow separation starts at the nose of the stenosis, where vortices are created. A rise in vorticity suggests that more vortex production is taking place. This will result in blood flow recirculation and stasis, as show in figure 8.

From figure 6 it is clear that the vorticity increases as the stenosis area increase, also at higher blood velocities the vorticity be bigger as result of increased body acceleration, physical exertion, and other factors.

4. Clinical Issues

4.1. Strain rate

For the cases that were analysed, the strain rate's clinical significance is presented with different conditions, noticing that the values of strain rate be higher when increase the flowrate as presented in figure 7. It should be noted that the narrowing region is where the strain rate has its maximum value, which is likely to produce hemolysis.

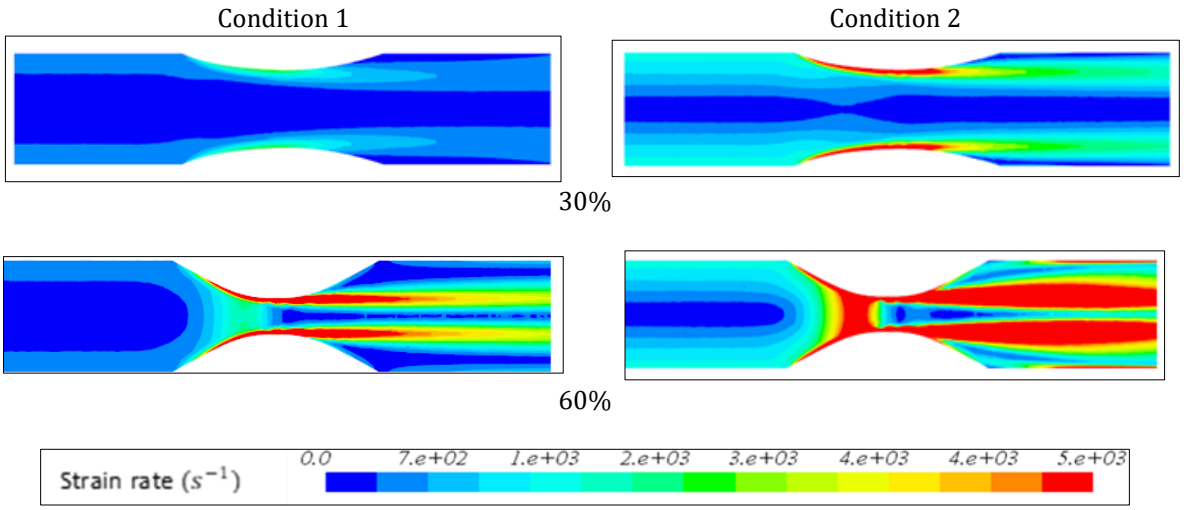

Figure 7 Contour of strain rate at mid plane

4.2. Wall Shear Stress (WSS)

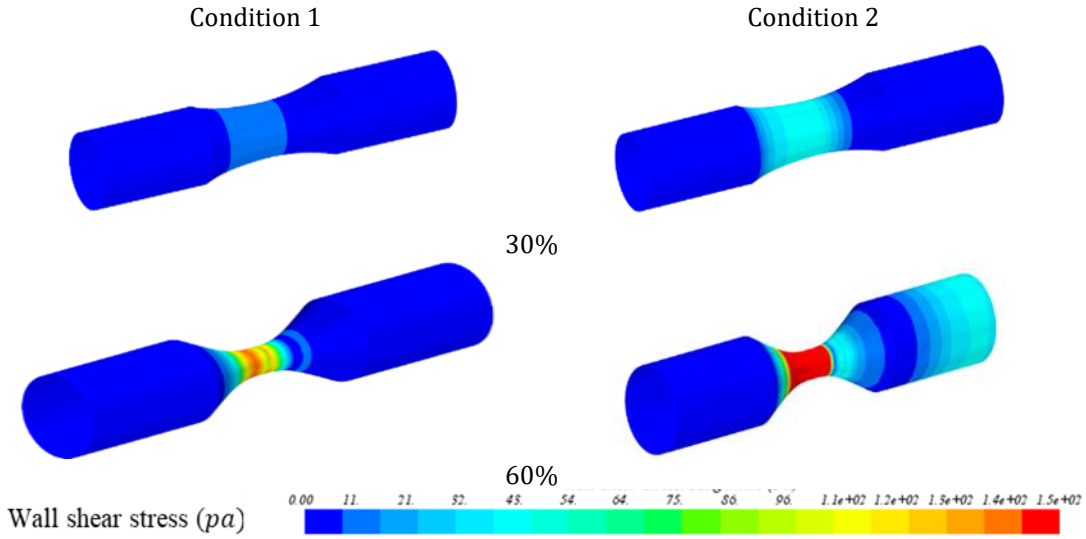

Figure 8 Contour of wall shear stress at the artery wall

The magnitude of WSS is presented at figure 8. The degree of stenosis has a big influence on the WSS outcomes. The temporal variations in hemodynamic loads exerted on artery wall are measured by the WSS gradient. The readings are

significantly higher in stenosed areas than in non-stenosed areas. The WSS magnitude distributions findings vary in the stenosis area/s comparing to unstenosed sections. WSS is highest at the neck (stenosis) and rises downstream following the stenoses as the flow becoming highly disrupted to the obstruction.

4.3. Effect of non-Newtonian

The local Importance Factor (IF) is examined to give a more quantitative measurement of the level of non-Newtonian effects within the device. The clinical significance of the IF for the instances studied is analysed as suggested by [15]

$$IF = \frac{\mu(S)}{\mu_\infty} \dots\dots\dots\dots\dots\dots\dots\dots (8)$$

Where;
$\mu(S)$ is the real dynamic viscosity of blood, which is specified by the non-Newtonian models,
μ_∞ denotes the Newtonian shear viscosity ($\mu_\infty = (0.00345\ pa.s)$

The Newtonian flow will have an IF equal to 1, while non-Newtonian flow zones will be indicated by values that are different from unity. As shown in figure 9 the IF be bigger in 30% stenosed artery than 60% stenosed artery, which mean that the $\mu(S)$ is higher than the μ_∞ , which mean that flow be non-Newtonian while in stenosed the flow be more Newtonian, and from these observations it can assume the flow be Newtonian for stenosed artery with high flow rate.

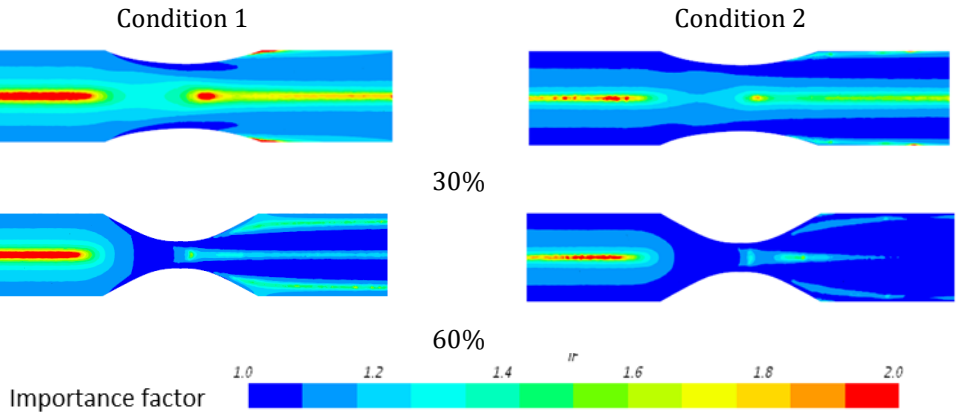

Figure 9 Contour of importance factor at mid plane

5. Conclusion

In the present simulation, two models of stenosed arteries were utilized to discuss the steady, turbulent blood flow with non-Newtonian properties utilizing the Carreau model. Through the use of Star-CCM+ software with various values of flow rates, the blood flow was simulated numerically in this model. Based on the results, an evaluation of the velocity vector, shear stress, viscosity, and strain rate revealed that the stenosed artery experiences more hemodynamic impacts as the flow rate increases, and the maximum change of these parameters occurs in the stenosed areas where there is a high blood flow velocity. Due to the smaller lumen diameter, the increased velocity causes greater blood flow resistance and reduced blood flow. This information could be extremely useful to medical professionals in locating hotspots where blood tends to collect. Furthermore, blood flow in the plaque-effected region is restricted, resulting in an imbalance in oxygen demand and supply in the tissue. Another of the main reasons for chest discomfort and other symptoms of coronary heart disease is the diminished oxygen delivery to the surrounding tissues.

Compliance with ethical standards

Disclosure of conflict of interest

No conflict of interest.

References

[1] S. Kamangar, "Numerical simulation of pulsatile blood flow characteristics in a multi stenosed coronary artery," Biomed. Mater. Eng., vol. 32, no. 5, pp. 309–321, 2021, doi: 10.3233/BME-211234.

[2] T. Chaichana, Z. Sun, and J. Jewkes, "Computational fluid dynamics analysis of the effect of plaques in the left coronary artery," Comput. Math. Methods Med., vol. 2012, no. December, pp. 12–16, 2012, doi: 10.1155/2012/504367.

[3] S. Fazli, E. Shirani, and M. R. Sadeghi, "Numerical simulation of LDL mass transfer in a common carotid artery under pulsatile flows," J. Biomech., vol. 44, no. 1, pp. 68–76, 2011, doi: 10.1016/j.jbiomech.2010.08.025.

[4] N. Ameer Ahamad, S. Kamangar, and I. A. Badruddin, "The influence of curvature wall on the blood flow in stenosed artery: A computational study," Biomed. Mater. Eng., vol. 29, no. 3, pp. 319–332, 2018, doi: 10.3233/BME-181734.

[5] X. Chen et al., "Hemodynamics in coronary arterial tree of serial stenoses," PLoS One, vol. 11, no. 9, pp. 1–13, 2016, doi: 10.1371/journal.pone.0163715.

[6] E. Boutsianis et al., "Computational simulation of intracoronary flow based on real coronary geometry," Eur. J. Cardio-thoracic Surg., vol. 26, no. 2, pp. 248–256, 2004, doi: 10.1016/j.ejcts.2004.02.041.

[7] M. X. Li, J. J. Beech-Brandt, L. R. John, P. R. Hoskins, and W. J. Easson, "Numerical analysis of pulsatile blood flow and vessel wall mechanics in different degrees of stenoses," J. Biomech., vol. 40, no. 16, pp. 3715–3724, 2007, doi: 10.1016/j.jbiomech.2007.06.023.

[8] C. Moreno and K. Bhaganagar, "Modeling of stenotic coronary artery and implications of plaque morphology on blood flow," Model. Simul. Eng., vol. 2013, 2013, doi: 10.1155/2013/390213.

[9] N. Beratlis, E. Balaras, B. Parvinian, and K. Kiger, "A numerical and experimental investigation of transitional pulsatile flow in a stenosed channel," J. Biomech. Eng., vol. 127, no. 7, pp. 1147–1157, 2005, doi: 10.1115/1.2073628.

[10] R. Trip, D. J. Kuik, J. Westerweel, and C. Poelma, "An experimental study of transitional pulsatile pipe flow," Phys. Fluids, vol. 24, no. 1, 2012, doi: 10.1063/1.3673611.

[11] T. Chaichana, Z. Sun, and J. Jewkes, "Haemodynamic analysis of the effect of different types of plaques in the left coronary artery," Comput. Med. Imaging Graph., vol. 37, no. 3, pp. 197–206, 2013, doi: 10.1016/j.compmedimag.2013.02.001.

[12] S. Kamangar et al., "Influence of stenosis on hemodynamic parameters in the realistic left coronary artery under hyperemic conditions," Comput. Methods Biomech. Biomed. Engin., vol. 20, no. 4, pp. 365–372, 2017, doi: 10.1080/10255842.2016.1233402.

[13] J. Janela, A. Moura, and A. Sequeira, "A 3D non-Newtonian fluid-structure interaction model for blood flow in arteries," J. Comput. Appl. Math., vol. 234, no. 9, pp. 2783–2791, 2010, doi: 10.1016/j.cam.2010.01.032.

[14] M. G. Rabby, S. P. Shupti, and M. M. Molla, "Pulsatile Non-Newtonian Laminar Blood Flows through Arterial Double Stenoses," J. Fluids, vol. 2014, pp. 1–13, 2014, doi: 10.1155/2014/757902.

[15] M. G. Al-Azawy, S. K. Kadhim, and A. S. Hameed, "Newtonian and non-newtonian blood rheology inside a model of stenosis," CFD Lett., vol. 12, no. 11, pp. 27–36, 2020, doi: 10.37934/cfdl.12.11.2736.

[16] B. M. Johnston, P. R. Johnston, S. Corney, and D. Kilpatrick, "Non-Newtonian blood flow in human right coronary arteries: Steady state simulations," J. Biomech., vol. 37, no. 5, pp. 709–720, 2004, doi: 10.1016/j.jbiomech.2003.09.016.

[17] M. M. Molla and M. C. Paul, "LES of non-Newtonian physiological blood flow in a model of arterial stenosis," Med. Eng. Phys., vol. 34, no. 8, pp. 1079–1087, 2012, doi: 10.1016/j.medengphy.2011.11.013.

[18] P. Halder, A. Husain, M. Zunaid, and A. Samad, "Newtonian and non-Newtonian pulsatile flows through an artery with stenosis," J. Eng. Res., vol. 14, no. 2, pp. 191–205, 2017, doi: 10.24200/tjer.vol.14iss2pp191-205.

[19] K. E. Hoque, M. Ferdows, S. Sawall, and E. E. Tzirtzilakis, "The effect of hemodynamic parameters in patient-based coronary artery models with serial stenoses: normal and hypertension cases," Comput. Methods Biomech. Biomed. Engin., vol. 23, no. 9, pp. 467–475, 2020, doi: 10.1080/10255842.2020.1737028.

[20] STAR-CCM+, "STAR-CCM+ Documentation Theory Guide, Turbulence," Siemens,GER, 2020.

[21] S. W. Levy, Use of Madribon in Dermatological Conditions, With Special Reference To Acne, vol. 82, no. 1. 1959.

[22] S. Li et al., "Numerical and experimental investigations of the flow–pressure relation in multiple sequential stenoses coronary artery," Int. J. Cardiovasc. Imaging, vol. 33, no. 7, pp. 1083–1088, 2017, doi: 10.1007/s10554-017-1093-3.

[23] A. Arzani, "Coronary artery plaque growth: A two-way coupled shear stress–driven model," Int. j. numer. method. biomed. eng., vol. 36, no. 1, pp. 1–12, 2020, doi: 10.1002/cnm.3293.

[24] S. K. Kadhim, M. G. Al-Azawy, S. A. G. Ali, and M. Q. Kadhim, "The influence of non-Newtonian model on properties of blood flow through a left coronary artery with presence of different double stenosis," Int. J. Heat Technol., vol. 39, no. 3, pp. 895–905, 2021, doi: 10.18280/ijht.390324.

[25] K. Manceau, R. and Hanjalic, "Elliptic blending model: A new near-wall Reynolds-stress turbulence closure," Phys. Fluids, vol. 2, pp. 744–754, 2002.

[26] R. Manceau, "Recent progress in the development of the Elliptic Blending Reynolds-stress model," Int. J. Heat Fluid Flow, vol. 51, no. September, pp. 195–220, 2015, doi: 10.1016/j.ijheatfluidflow.2014.09.002.

[27] P. Hariharan et al., "Multilaboratory particle image velocimetry analysis of the FDA benchmark nozzle model to support validation of computational fluid dynamics simulations," J. Biomech. Eng., vol. 133, no. 4, pp. 1–14, 2011, doi: 10.1115/1.4003440.

[28] M. G. M. Al-azawy, "Evaluation of recently developed computational fluid dynamics techniques for the assessment of blood flow inside different heart pumps," 2016.